Changes in Molecular Dynamics during Bulk Polymerization of an Epoxide−Amine System As Studied by Dielectric Relaxation Spectroscopy

Jérôme Fournier, Graham Williams,* Christine Duch, and George Anthony Aldridge

Department of Chemistry, University of Wales, Swansea, Singleton Park, Swansea SA2 8PP, United Kingdom

Received December 4, 1995; Revised Manuscript Received July 24, 1996[⊗]

ABSTRACT: Dielectric relaxation spectroscopy (DRS) and differential scanning calorimetry (DSC) have been used simultaneously as a means of following the isothermal cure of the diglycidyl ether of Bisphenol A with 4,4′-diaminodicyclohexylmethane in the temperature range 290−353 K. The dielectric permittivity and dielectric loss of the thermosetting mixture have been measured as a function of reaction time over the frequency range $10^{1.2}$−10^5 Hz. The evolution of the dielectric properties was studied as the curing temperature was lowered to values close to the solidification of a sample. The kinetics of the cure have also been determined, using calorimetry, for four reaction temperatures over the whole range of conversion up to the point where the system vitrifies and the reaction becomes diffusion-controlled. Correlations between the changes in molecular dynamics and the chemical kinetics occurring during the thermosetting process have been made in some detail, and a theoretical working model has been developed that allows DRS to predict the course of the reaction in the vitrification range. Previous interpretations of dielectric events in this vitrification region, based on experimental kinetic and dielectric results, are reexamined.

1. Introduction

Glass-forming systems, such as molecular liquids or amorphous polymers, exhibit different relaxation phenomena in the glass transition range which arise from the translational and reorientational motions of the molecules. They have been studied for many years using a variety of physical techniques including those of dynamic mechanical,[1,2] nuclear magnetic resonance, and dielectric relaxation.[1,3−7] In dielectric relaxation spectroscopy (DRS) the complex dielectric permittivity $\epsilon(\omega,t_r)$ at a frequency $f = \omega/2\pi$ and a reaction time t_r, may be used to monitor the course of chemical reactions.[8−15] During the isothermal curing of a diamine/diepoxide system, the epoxide groups open to form a linkage with the amine groups[16,17] and the reaction proceeds relatively slowly toward vitrification. At long times, the diffusion control of the reacting groups, arising from the densification and increasing viscosity of the network during the vitrification, retards substantially the polymerization process, and the reaction effectively "stops". The dielectric properties of a system change as the reaction progresses and these changes correspond to (i) a change in the dipole moment per unit of monomer in the mixture, resulting from the disappearance of epoxide and primary amine groups and the appearance of new groups and (ii) an increase in the average dielectric relaxation time of the material due to a decrease in the molecular mobility in the medium as the network is forming. Dielectric experiments give information on the molecular chain dynamics at given reaction times and hence on the evolution of the molecular mobility of the polymer molecules during the curing process but do not give direct indications of the extent of reaction α. Dielectric and mechanical properties of a thermoset cure are normally each used on their own to predict the approach of vitrification, which involves several assumptions in the absence of simultaneously obtained chemical data. Sheppard and Senturia[6] have reviewed the different empirical approaches which attempted to link the kinetic and the dielectric data for epoxide−amine thermosetting systems. They concluded that most of these were based on unjustified assumptions and failed because of oversimplifications of the chemical kinetics or because of invalid interpretation of dielectric events. The kinetic characteristics of the thermosets (e.g. diepoxide/diamine) are now well understood[16,18] and a rather complex model was recently proposed by Cole,[17] which describes the cure kinetics of epoxide−amine thermosetting resins over the entire range of α taking in account all the reactions, including etherification.

In this work, we give extensive dielectric data for epoxide−amine thermosetting systems at different reaction temperatures which were determined over a range of frequency and time *cumulatively* during the reaction. In addition, we have made simultaneous complementary studies of the thermochemistry in real time for reactions at different temperatures. By combination of the dielectric and thermochemical data, we have established a new comprehensive correlation model of dielectric properties during a thermoset cure of the diepoxide−diamine system, including an improved model for chemical kinetics and an improved relation between state of cure, temperature, and various dielectric parameters that were contained in earlier studies. The representation of such a model, built on a few clear working assumptions, provides a general trend for the variation of dielectric parameters (e.g. the frequency of maximum dielectric loss) as the extent of reaction increases. This work allowed us to reexamine the interpretation of dielectric events which were widely used previously in the literature having basic assumptions without adequate verification.

2. Experimental Section

2.1. Sample Preparation. Diglycidyl ether of Bisphenol A (DGEBA) was provided by Shell Resins under the trade name Epikote 828, having MW = 340. The 4,4′-diaminodicyclohexylmethane (PACM) was obtained from Aldrich Chemical Co. All chemicals were used as received. The sample was

[⊗] Abstract published in *Advance ACS Abstracts,* September 15, 1996.

S0024-9297(95)01786-4 CCC: $12.00

prepared by mechanically mixing 2 mol of DGEBA with 1 mol of PACM during 5 min at 293 K.

2.2. Dielectric Measurements. The liquid epoxy mixture was simply sandwiched between the parallel-electrode dielectric cells which consist of two, strictly flat brass disks separated by two 0.12 mm thick PTFE spacers. Then the cell was set up in an enclosed chamber and the electrodes were linked to the Digibridge (see below). Simple contacts between the top part of the cell and the top electrode allows the sample to be connected to the dielectric assembly.

The empty cell capacitance C_0 was found to be approximately constant with the measurement frequency, at a value equal to 36.5 pF. The theoretical value for C_0 was 36.2 pF. The deviation between the measured and the calculated value was less than 1%, arising from the contributions of the spacers and the edge capacitance. The value of the loss index $G_p(\omega)/\omega$ for the empty cell was approximately equal to 0.01 pF for all the measurement frequencies. The small variations were assumed to result from the noise, and they do not affect the calculation and the interpretation of the following results.

The enclosed chamber was placed into a water bath (Techne, Cambridge) during the experiment, and a Techne TU-160 thermoregulator was used to control the temperature of the water in the working range 288−353 K. The dielectric permittivity and dielectric loss were measured at 20 frequencies in the range from 12 Hz to 200 kHz. The measurements of equivalent sample parallel capacitance $C_p(\omega)$ and loss index G_p/ω, where G_p is the sample conductance and $\omega = 2\pi f$/Hz, were taken every 2 min across the entire frequency range, and the times of measurement corresponding to *each* of the measurement data points were stored for the 20 frequencies scanned. The dielectric spectrometer was a 1693 RLC GenRad Digibridge interfaced with a Hewlett-Packard 915 3C computer for automatic data acquisition. Such data were post-processed to yield 2D plots of ϵ' and ϵ'' vs time at fixed frequency of measurement, ϵ' and ϵ'' vs log(f) at fixed time of measurement, and 3D plots of ϵ' and ϵ'' vs log(f) and time. Here ϵ' and ϵ'' are the real and imaginary parts of the complex dielectric permittivity ϵ.

2.3. Kinetic Measurements. A Stanton Redcroft STA 625 differential scanning calorimeter (DSC) was used in conjunction with a PL Thermal Science data acquisition system for all the thermokinetic studies. The instrument was calibrated prior to the set of experiments, using the melting temperatures of pure indium (156.60 °C) and tin (231.88 °C), and a base line calibration was also accomplished by scanning without a sample up to a desired temperature, to check that the scan was free of any peaks or discontinuities due to impurities. The thermal analysis consisted of an isothermal DSC run followed by a dynamic run. Approximately 50 mg of sample deriving from the same epoxy mixture used for the simultaneous dielectric measurements was placed in a standard aluminum crucible and placed in the microbalance. The reference was an empty aluminum crucible. The sample was heated in an air atmosphere from 288 to the experimental temperature at the fixed rate of 10 K/min, and the calorimeter signal (heat flow = dQ/dt) was recorded by the computer every 2 min during the isothermal polymerization. When the heat flow had reached a constant value corresponding to the end of the exothermic reaction, the sample was then cooled to 288 K. Then a heating run was performed to 523 K at a suitable temperature increase rate (5 K/min), allowing the determination of the residual heat of polymerization Q_r for all the samples. The residual heat of cure Q_r is evolved when a cured sample is heated above its glass transition temperature, which, for the samples prepared here, approximates to T_R, the reaction temperature. In this type of cure, the heat evolved is directly proportional to the number of epoxide groups reacted,[16,19] so the extent of reaction $\alpha(t)$ is given by the following equation:

$$\alpha(t) = \alpha_0 + \left[\frac{1-\alpha_0}{Q_i + Q_r}\right] Q(t) \tag{1}$$

where $Q(t)$ is the heat produced by the reaction at the time t:

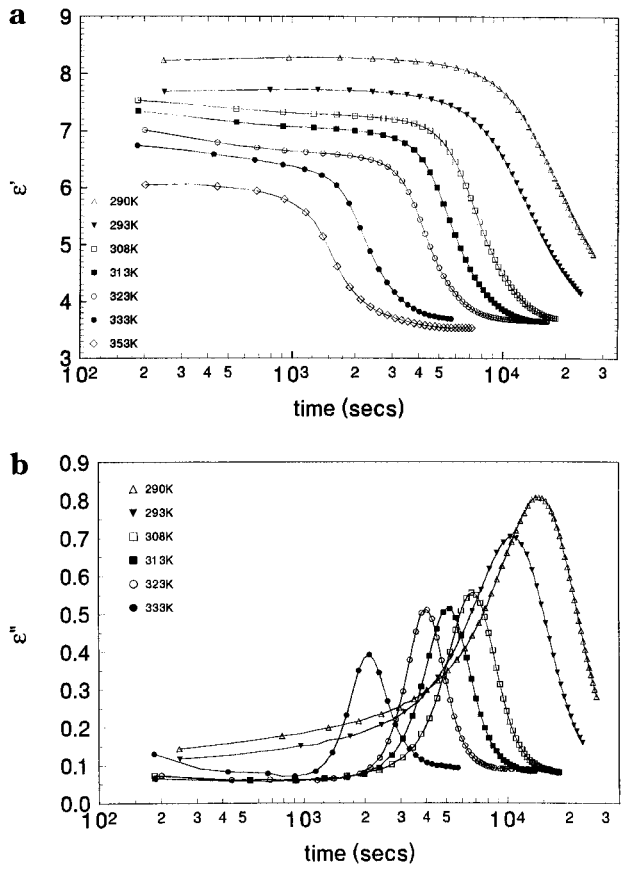

Figure 1. (a) Permittivity $\epsilon'(\omega,t_r)$ against the reaction time t_r, on a logarithmic scale, for the thermoset DGEBA−PACM at the measurement frequency $f = 10^5$ Hz for seven different temperatures in the range 290−353 K. (b) Loss factor $\epsilon''(\omega,t_r)$ against the reaction time t_r, on a logarithmic scale, for the thermoset DGEBA−PACM at the measurement frequency $f = 10^5$ Hz for six different temperatures in the range 290−333 K.

$$Q(t) = \int_0^t \frac{dQ}{dt}\, dt \tag{2}$$

Q_i is the total heat evolved during the isothermal polymerization at $T = T_R$, and Q_r is the residual heat of cure determined as described above. α_0 is the extent of reaction at the beginning of the cure. α_0 was found to be negligible and the expressions of α and dα/dt as a function of time are reduced to

$$\alpha(t) = \frac{Q(t)}{Q_i + Q_r} \tag{3}$$

$$\frac{d\alpha}{dt} = \left[\frac{1}{Q_i + Q_r}\right]\frac{dQ}{dt} \tag{4}$$

Equations 3 and 4 were used to determine $\alpha(t)$ and dα/dt for epoxide−amine reactions at four reaction temperatures.

3. Dielectric Data

The aim of our dielectric experiments was to monitor the permittivity $\epsilon'(\omega,t_r)$ and loss factor $\epsilon''(\omega,t_r)$ at different measuring frequencies $f = \omega/2\pi$ and reaction times t_r for a fixed reaction temperature T_R. Experiments were conducted at eight temperatures between 290 and 353 K. As one example, Figures 1a and 1b show ϵ' and ϵ'' vs $\log_{10}(t_r)$ at the fixed frequency of 10^5 Hz for these eight temperatures. In the initial plateau region $\epsilon'(\omega,t_r,T_R)$ is the static permittivity $\epsilon_0(T_R)$, which is approximately independent of t_r but decreases with

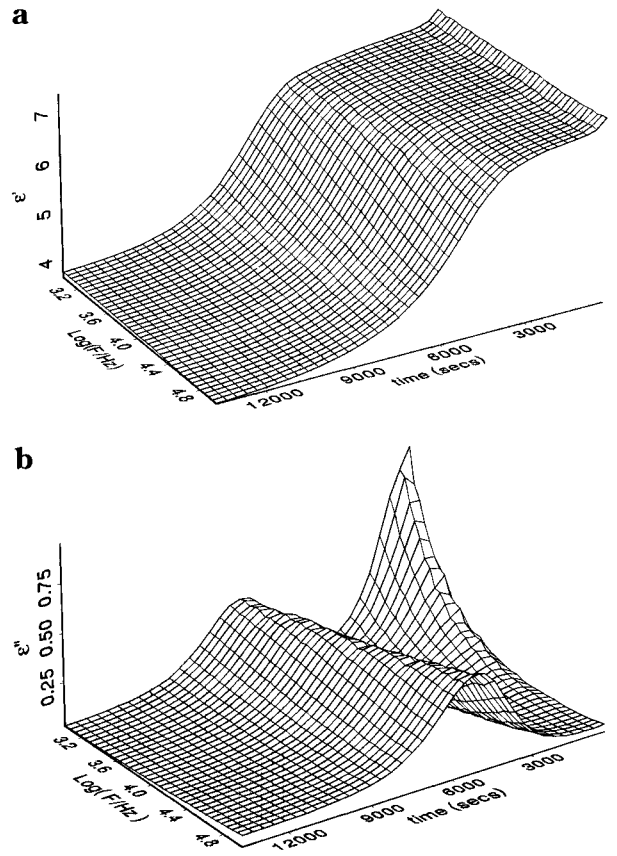

Figure 2. (a) Three-dimensional plots of the dielectric permittivity $\epsilon'(\omega,t_r)$ against the time and the frequency, on a logarithmic scale, for the thermoset DGEBA−PACM at the cure temperature $T = 313$ K. (b) Three-dimensional plots of the dielectric loss factor $\epsilon''(\omega,t_r)$ against the time and the frequency, on a logarithmic scale, for the thermoset DGEBA−PACM at the cure temperature $T = 313$ K.

increasing temperature T_R. At longer times, $\epsilon'(\omega,t_r)$ exhibits a fall from a liquid to a glassy polymer value, reaching the "unrelaxed" permittivity ϵ_∞. As T_R is increased, this dispersion region moves to shorter times, reflecting the decreased times required for glass formation with respect to this fixed measuring frequency. The loss data $\epsilon''(\omega,t_r,T_R)$ are shown in Figure 1b and are complementary to the data of Figure 1a. The process moves to shorter times and the peak height decreases as T_R is increased. The behavior shown in Figures 1a and 1b is similar to that observed for other epoxide−amine thermosetting systems.[6−15] The ability of the measuring system to acquire data of this kind over a range of frequencies enabled us to make similar plots to those in Figure 1 at the other 19 frequencies measured during an experiment. The plot of ϵ'' vs t_r (or $\log_{10}(t_r)$) exhibits a maximum at $t_r = t_m$ for each measuring frequency at a given reaction temperature T_R. Numerical analysis of the plots in Figure 1b allowed values of t_m to be determined at each of the 20 frequencies in each run, allowing Figure 3 to be constructed. Our permittivity and loss data could also be presented in 3D form, as shown in Figures 2a (for the permittivity) and 2b (for the loss factor), at 313 K as one example. Similar plots were obtained at the other reaction temperatures. In Figure 2a, the permittivity falls from its short-time plateau value through the relaxation region as the material appears to become a glass, with respect to this frequency of measurement. The complementary loss data in Figure 2b show a short-time low-frequency region of loss due to ionic species and a well-defined loss

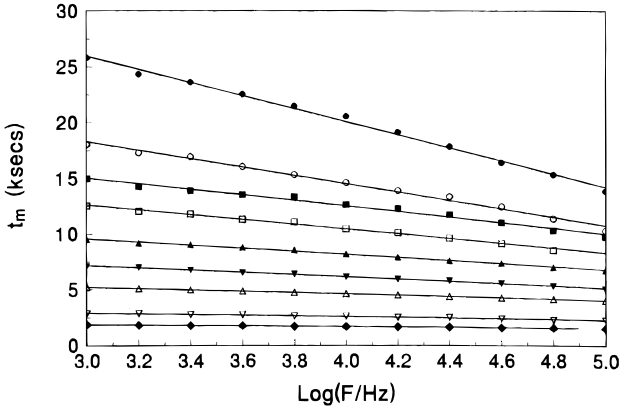

Figure 3. Time of maximum loss t_m against the frequency, on a logarithmic scale. Here shown are t_m for the thermoset DGEBA−PACM at the cure temperatures $T = 290$ K (●), $T = 293$ K (○), $T = 298$ K (■), $T = 303$ K (□), $T = 308$ K (▲), $T = 313$ K (▼), $T = 323$ K (△), $T = 333$ K (▽), and $T = 353$ K (◊).

peak whose frequency location changes systematically, moving to lower frequencies as the reaction proceeds. 3D representations of the dielectric behavior during reaction of a related epoxy−amine system have been shown previously by Maistros and co-workers.[15] Figure 3 shows the values of the time of maximum loss factor t_m as a function of measuring frequency for different reaction temperatures derived from Figure 2b. Only a portion of our data is shown, but even then, Figure 3 contains the values of t_m determined from 90 plots of $\epsilon''(\omega,t_r,T_R)$ vs t_r at fixed ω and T_R. Such data could not easily be obtained before the advent of modern semi-automatic dielectric spectrometers of the kind used for this study.

The dielectric behavior seen in Figures 2a and 2b arises from dipolar and ionic species whose concentration and reorientational dynamics (for dipoles) and translational dynamics (for ions) change with time as a result of chemical reaction. We may write

$$\epsilon(\omega,t_r) = \epsilon'(\omega,t_r) - i\epsilon''(\omega,t_r) - i\epsilon''_i(\omega,t_r) \qquad (5)$$

where ϵ' and ϵ'' contain contributions from dipolar species and ϵ''_i is the contribution from ionic species. For a simple conductivity process, $\epsilon''_i = \sigma/\omega\epsilon_0$, where ϵ_0 is the permittivity of free space. The rising loss at low frequencies and short times in Figure 2b is due to ionic species, but ϵ''_i follows a power law $\epsilon''_i \sim \omega^{-n}$, which may be rationalized in terms of hopping or dispersive models of ion transport.

The short-time behavior of ϵ' in Figure 1a gives the static permittivity $\epsilon_0(t_r)$, which is expressed as a function of the sum of the concentration and average squared dipole moments, c_i and $\langle\mu_i^2\rangle$, respectively, of the different species in the mixture at the time t_r:

$$\epsilon_0(t_r) = \epsilon_\infty + F(\epsilon_0,\epsilon_\infty)\sum_i c_i \frac{\langle\mu_i^2\rangle}{kT} \qquad (6)$$

ϵ_∞ is the limiting high-frequency permittivity of the material and $F(\epsilon_0,\epsilon_\infty)$ takes into account the relation between applied and local electric fields.[1] $\langle\mu_i^2\rangle$ refers to the mean square dipole moment of amine (primary and secondary), hydroxyl, and ether groups present in the mixture. $\epsilon_0(t_r)$ shows only small variations with t_r (see e.g. Figures 1a and 1b), so replacement of reactant dipoles with product dipoles during reaction gives only a small variation in $\sum c_i\langle\mu_i^2\rangle$ in eq 6. Increase in reaction

Table 1. Dielectric Parameters Observed for the Measurement Frequency $f = 10^5$ Hz during the Cure of the Epoxide−Amine Thermoset[a]

T (K)	ϵ_0	$\Delta\epsilon$	$t_m \times 10^{-3}$ (s)	ϵ''_{max}	HW (s^{-1})	area (s^{-1})	$k \times 10^4$ (s^{-1})	$f_m(0)$ (Hz)	r
290	8.30	4.60	13.90	0.809	17820	13560	3.90	0.26×10^8	0.997
293	7.80	4.00	10.30	0.703	12670	7550	6.00	0.69×10^8	0.995
303	7.70	3.90	8.35	0.644	7440	4330	8.90	8.70×10^8	0.992
308	7.25	3.55	6.80	0.556	5040	2800	10.60	7.70×10^8	0.997
313	7.05	3.35	5.10	0.515	3630	1830	16.60	86.0×10^8	0.997
323	6.78	3.08	4.05	0.510	2170	925	22.80	126×10^8	0.998
333	6.50	2.80	2.30	0.391	1280	468	72.30	135×10^{10}	0.984
353	6.00	2.40	1.50	0.221	470	142	220.2	990×10^{10}	0.990

[a] T is the temperature of the cure, ϵ_0 is the relaxed permittivity, $\Delta\epsilon$ is the total decrease of permittivity, which can also be written ($\epsilon_0 - \epsilon_\infty$), t_m is the time of maximum loss, and ϵ''_{max} is the height of the loss peak and HW its half-width, both of which have been measured on plots ϵ'' vs t not shown in this article. The seventh column displays the area of the loss peak, which was also determined from a plots ϵ'' vs t (in a linear scale). k and $f_m(0)$ are the temperature-dependent constants included in eq 8: $f_m = f_m(0) \exp(-kt_m)$. The correlation coefficient r, in the last column, corresponds to Figure 3, where t_m is drawn as a function of $\log(f_m)$.

temperature gives a decrease in the relaxation strength $\Delta\epsilon = \epsilon_0(t_r) - \epsilon_\infty$. In contrast, $\epsilon_0(t_r)$ in the short-time plateau region in Figure 1a decreases with increasing reaction temperature. Equation 6 predicts that $\Delta\epsilon = \epsilon_0 - \epsilon_\infty$ should be inversely proportional to temperature (K), and, taking $\epsilon_\infty \sim 3.5$, this is true, approximately, for our data.

The relaxation behavior seen in Figures 1 and 2 arises from the changes in molecular mobility of the dipoles in the mixture as a liquid is transformed to a glass through the bulk-polymerization process. The dielectric parameters determined from our studies are summarized in Table 1. The values of $\Delta\epsilon$ have a limited accuracy because ϵ_∞ is difficult to evaluate for the lower curing temperatures. At 290, 293, and 303 K the value of ϵ_∞ is determined by extrapolation as the average value of ϵ_∞ of the other experiments, for which the unrelaxed permittivity is relatively constant and does not depend upon the final degree of conversion of the polymer. The characteristic dipolar loss peaks are displayed in Figure 1b for different experimental temperatures, arising from the energy loss principally entailed by dipole motion when the network becomes a glass. It can be described satisfactorily if the three following parameters are known: t_m, the time of maximum loss; ϵ''_{max}, the height of the peak; HW, its half-width. These parameters are displayed in Table 1. The observed decrease in t_m, ϵ''_{max}, and HW, obeying approximately the Fuoss−Kirkwood equation,[1] is a reflection of an irreversible thermally activated chemical reaction. The origin and the theoretical analysis of these changes in the real and the imaginary parts of the complex permittivity have been studied in detail in several previous publications. In our case, we are interested in studying the dielectric properties of the epoxide−amine thermoset with the aim of establishing relations between dielectric parameters and chemical events and the vitrification or the degree of polymerization.

We chose to use the time of maximum loss ϵ'' to define an operational curing time with respect to measuring frequency and we called it t_m. The values of t_m were plotted against frequency for different experimental temperatures in Figure 3, and t_m was found to be linearly dependent on $\log(f/\text{Hz})$ in our range. Following Lane and Seferis,[20] we write

$$\tau = \tau_0 \exp(kt_m) \tag{7}$$

where τ_0 is the relaxation time for the uncured material, k is a constant for a given reaction temperature, and t_m is the time of maximum loss for a given frequency of measurement. Insofar as the frequency of maximum loss f_m can be related to the average relaxation time with

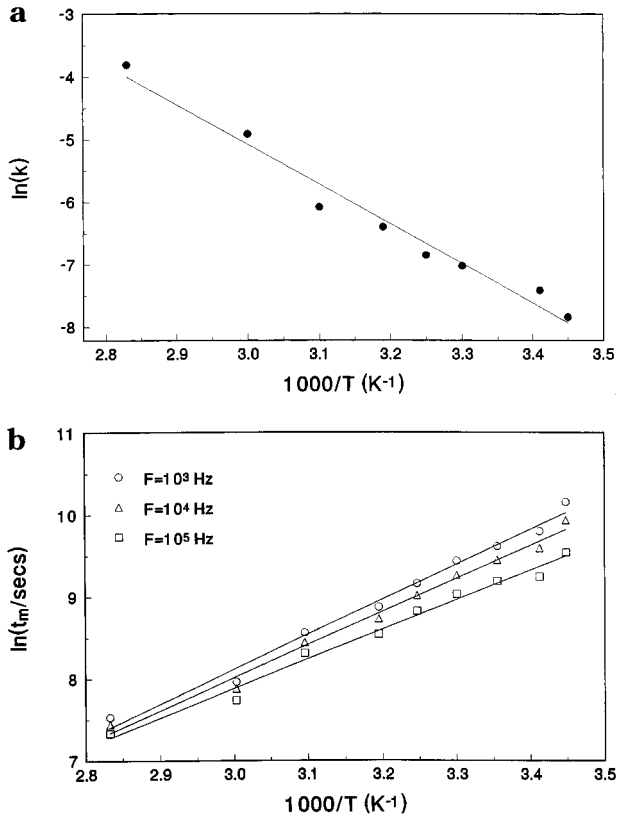

Figure 4. (a) ln(k) and (b) $\ln(t_m/s)$ against reciprocal temperature. k is an empirical constant in eqs 7 and 8, and t_m is the time of maximum loss.

the equation $f_m = 1/(2\pi\tau)$, Mangion and Johari[14] have rewritten eq 7 as

$$f_m = f_m(0) \exp[-kt_m] \tag{8}$$

Good straight-line plots show that eq 8 gives a good representation of our data, where both $f_m(0)$ and k depend upon the reaction temperature. Table 1 shows the increase of k as the temperature is increased. The plots of k as a function of reciprocal of temperature of cure are drawn in Figure 4a and they are found to lie on a straight line with a good linear correlation coefficient $r = 0.99$. Thus k may be considered to obey the Arrhenius law as

$$k = k_0 \exp\left(\frac{-Q_{app}}{RT}\right) \tag{9}$$

where Q_{app} is an apparent activation energy, R is the gas constant, and k_0 is the value of k for infinite

temperature. We found $\ln(k_0) = 14.0$, where k_0 is expressed in s^{-1} and $Q_{app} = 764$ kJ/mol. Thus the frequency of maximum loss is found to follow "first-order kinetics" as indicated by eq 8 with a rate coefficient k obeying an Arrhenius law. In this case, the influence of the temperature in the change of t_m is implicit.

Another approach is to consider a direct relationship between the time of maximum loss and the temperature of the cure, based on the kinetic theory[16,18] of polyaddition reactions of epoxide with amine. Mangion and Johari[12,21] proposed that the time Δt necessary for the thermosetting material to reach a predefined extent of reaction or a particular physical state varies with the temperature and can be given approximately by the equation

$$\Delta t(T) = \Delta t_0 \exp\left(\frac{E}{RT}\right) \tag{10}$$

Mangion and Johari assumed that the time of maximum loss for a fixed measuring frequency may characterize a certain extent of reaction and they used $\Delta t = t_m$ in eq 10, where E corresponds to an activation energy and Δt_0 is the extrapolated value of t_m when the curing temperature becomes infinite. The values of t_m corresponding to the present thermoset epoxide−amine reaction are plotted in Figure 4b against the reciprocal of T_{cure} for three fixed measurement frequencies. The calculation of E has been carried out for 12 measurement frequencies in the range 10^3-10^5 Hz and the mean value of E at 99% confidence level was found to be 38.2 $\pm$ 2.9 kJ mol^{-1}. Mangion and Johari[10] studied different systems and they obtained $\Delta t_0 = 668$ μs and $E = 47.1$ kJ mol^{-1} for the DGEBA−DDM thermoset and $\Delta t_0 =$ 56.4 ms and $E = 44.5$ kJ mol^{-1} for the DGEBA−DDS thermoset at $f = 10^3$ Hz, where DDM is 4,4′-diaminodiphenylmethane and DDS is 4,4′-diaminodiphenyl sulfone. Our data are very similar. They show that Δt_0 increases significantly with the frequency of measurement and the apparent activation energy E may also be considered as a frequency-dependent variable. Thus the significance of eq 10 can be queried insofar as the main parameters of this relation are obviously linked with the measurement frequency. The concept of accumulated equivalent curing time yielding eq 10 is based on the main assumption[21] that the reaction path is the same at all temperatures, and it tends to relate the time Δt required to reach a predefined extent or a chemical and physical state with the temperature of the cure. The parameters Δt_0 and E must be independent of the spectroscopic technique of measurement used to determine them. Since Δt_0 and E are found to be obviously dependent on the measurement frequency in DRS as seen in Figure 4b, eq 10 is only valid for a fixed frequency of measurement. It is difficult to see an interpretation from a chemical or kinetic point of view. We also consider that no dielectric event associated with the extent of reaction has yet been established since t_m is strictly defined as the time required for the loss factor to reach a maximum for the fixed frequency f_m. Then the concept of accumulated equivalent curing time is not appropriate to the analysis of dielectric quantities such as the time of maximum loss, which does not define a chemical state independent of the measurement frequency. So the dielectric parameter t_m has to be considered as a two-variable function, taking in account the temperature and the frequency of measurement. A three-dimensional plot in Figure 5 presents our experimental data obtained for nine temperatures in the range

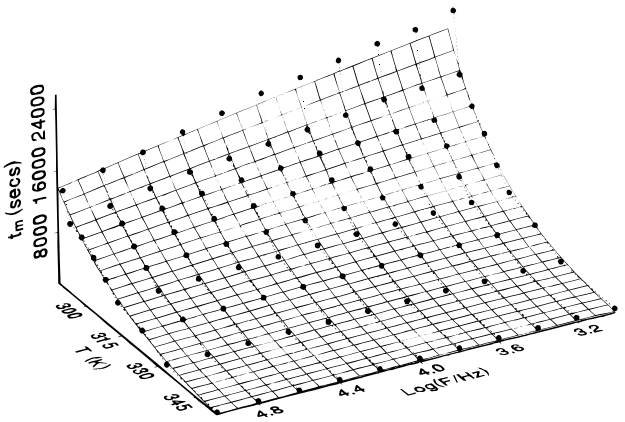

Figure 5. Time of maximum loss t_m against the temperature of cure and the frequency of measurement, on a logarithmic scale.

290−353 K and for eleven frequencies of measurement. At a fixed frequency, t_m is seen to increase exponentially with decreasing temperature. These results represent a good approximation until the temperature is lowered to around 293 K. Afterward the experimental data deviate strongly from the theoretical fitting curve, whose equation can be written as

$$t_m = t_{m0}(f_m) \exp[\delta(f_m)T] \tag{11}$$

where $t_{m0}(f_m)$ and $\delta(f_m)$ are two coefficients depending on the frequency of measurement. Measurements below 293 K are extremely difficult to perform because of the crystallization of the diamine ($T_{me1} = 288$ K) and the very high viscosity of the epoxide at this temperature, which make complete mixing of the components by manual means in a reasonable time almost impossible. Thus the reaction is diffusion controlled as soon as it starts and the time of maximum loss increases strongly with decreasing temperature for all the measurement frequencies. At low temperatures, the progress of the cure, in practice, depends upon the duration and the method of mixing the diepoxide with the diamine, and large variations of t_m can be observed for the same experimental conditions. Above 293 K, t_m obeys eq 11 satisfactorily and the two parameters have been determined using 11 frequencies of measurement:

$$t_{m0}(f_m) = 72670 - 9800 \times \log(f_m) \qquad (r = 0.997)$$

$$\delta(f_m) = -0.051 + 0.0030 \times \log(f_m) \qquad (r = 0.998)$$

The deviation between experimental data and the theoretical 3D curves is shown in Figure 5 and demonstrates that eq 11 gives a good fit of the behavior of t_m as a function of T_{cure} until a limit temperature around 293 K.

4. Thermochemical Data

The thermochemical studies give the conversion $\alpha(t_r)$ as a function of t_r at each reaction temperature. Our results are shown in Figure 6 and will be discussed further below.

To model the cure kinetics of epoxy−amine thermosetting systems, it is necessary to derive an equation expressing $d\alpha/dt$, the rate of change of conversion α with time, as a function of α and temperature. Sheppard and Senturia[6] related different analysis using the following differential equation to describe an isothermal cross-linking kinetics:

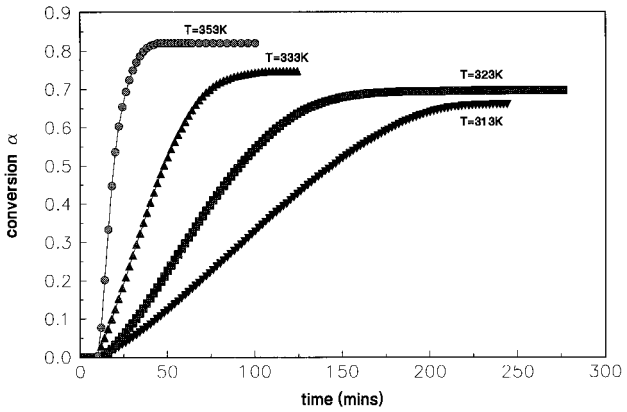

Figure 6. Extent of reaction α against the time of reaction (in minutes) for the curing temperatures T = 313 K (▽), T = 323 K (○), T = 333 K (▲), and T = 353 K (△).

$$\frac{d\alpha}{dt} = k(1-\alpha)^m \tag{12}$$

where k is the rate coefficient and m is the empirical reaction order. However, one difficulty with such empirical approaches is that they tend to oversimplify the chemical kinetics. In 1970, Horie et al.[22] proposed the following equation to describe the kinetics of polymerization of a resin epoxy and an amine:

$$\frac{d\alpha}{dt} = (k_1 + k_2\alpha)(1-\alpha)(B-\alpha) \tag{13}$$

where k_1 is a rate constant for the reaction catalyzed by groups initially present in the resin, k_2 is the rate constant for the reaction catalyzed by newly formed hydroxyl groups, and B is the ratio of primary amine N−H bonds to epoxide groups in the initial mixture. They[22] concluded that the curing reaction of DGEBA with aliphatic diamines, which proceeded through a third-order mechanism, was followed by the diffusion-controlled mechanism at the later stage of conversion, and the reaction ceased at the conversion where any segmental diffusion of functional groups was suppressed because of the onset of the glass transition of the system. Similar equations[11,23] were used for the thermosetting reactions of different systems DGEBA−diamine systems but they do not consider the reactions occurring in the later stage of the cure, such as the ether reaction,[18] which is believed to become particularly significant at high temperatures. Kamal[24] proposed the following semiempirical equation, taking in account etherification reactions:

$$\frac{d\alpha}{dt} = (k_1 + k_2\alpha^m)(1-\alpha)^n \tag{14}$$

Many workers[19] have proposed different values of the empirical reaction orders m and n. Cole[16] found that the values of n and m varied significantly with temperature. He developed recently a more rigorous model for describing the cure kinetics of general epoxy−amine systems. He concluded that the reaction could be divided into two stages. At the beginning of the cure, the amine−epoxide reaction dominates and the effect of the etherification reaction is insignificant, so the Horie[22] equation (13) is valid for the initial reaction. But in the later stages of curing, the isothermal cross-linking reaction tends to become simply first order with respect to epoxide concentration and can be described in terms of the simple differential equation

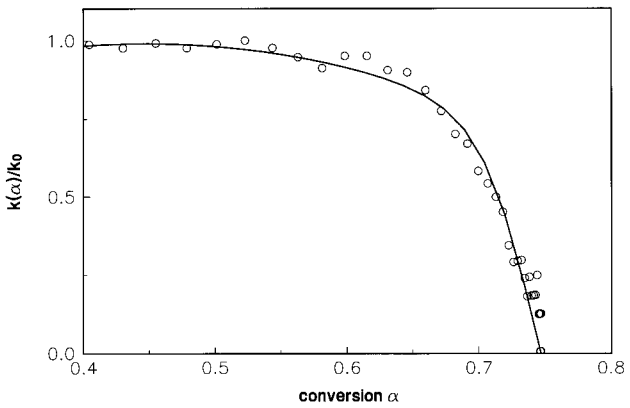

Figure 7. Normalized kinetic rate $k(\alpha)/k_0$ against the extent of reaction α during the later stages of the cure of the system DGEBA−PACM at T = 333 K.

$$\frac{d\alpha}{dt} = k(\alpha)(1-\alpha) \tag{15}$$

Here the rate coefficient $k(\alpha)$ is dependent upon the extent of reaction and will fall substantially when the reaction becomes diffusion controlled toward the end of the cure. Cole expressed this "diffusion factor" as

$$k(\alpha) = \frac{k_c}{1 + \exp[C(\alpha - \alpha_c)]} \tag{16}$$

In eq 16 the denominator is a cut-off function, which we note is formally the same as the Fermi−Dirac function in the band theory of metals. It allows $k(\alpha)$ to be constant for $\alpha < \alpha_c$ and to decrease rapidly to zero for $\alpha > \alpha_c$. Equation 16 gives a point of inflection for $k(\alpha)$ at $\alpha = \alpha_c$. Physically, it is more acceptable to expect that $-dk(\alpha)/d\alpha$ should increase monotonically in the diffusion-controlled regime. Therefore we modified Cole's equation (16) as follows:

$$f_d(\alpha) = \frac{k(\alpha)}{k_0} = 2\left[\frac{1}{1 + \exp[(\alpha - \alpha_f)/b]} - \frac{1}{2}\right] \tag{17}$$

In this equation, k_0 is the rate coefficient for non-diffusion-controlled kinetics, which is given by experiment for $0.4 < \alpha < 0.55$, where $(d\alpha/dt)/(1-\alpha)$ is approximately constant. Equation 17 is different from Cole's equation in the following ways:

(i) α_f is the final degree of polymerization, which is an experimental result ($\alpha_f = Q_i/(Q_i + Q_r)$), whereas α_c is a certain critical value that is difficult to determine with accuracy.

(ii) Equation 17 allows us to fit the experimental data to the final degree of conversion α_f as seen in Figure 6.

The constant b is the only unknown in eq 17, and it can be easily calculated in our case to give the best correlation coefficient between the theoretical curve and the experimental data that were obtained using DSC at four curing temperatures ranging from 213 to 253 K. The results in Figures 7−9 were derived from the DSC data presented in Figure 6, where the values of α, plotted with respect to the time of cure, describe typical curves characterizing an autocatalytic polymerization reaction. Figure 7 shows a normalized plot of the rate coefficient in the later stages of the cure at 333 K. We see that $k(\alpha)/k_0$ decreases dramatically for $\alpha > 0.65$ as the network vitrifies and the reaction becomes diffusion controlled. This behavior is observed in Figures 8 and 9 at respectively 323 and 353 K for high values of α.

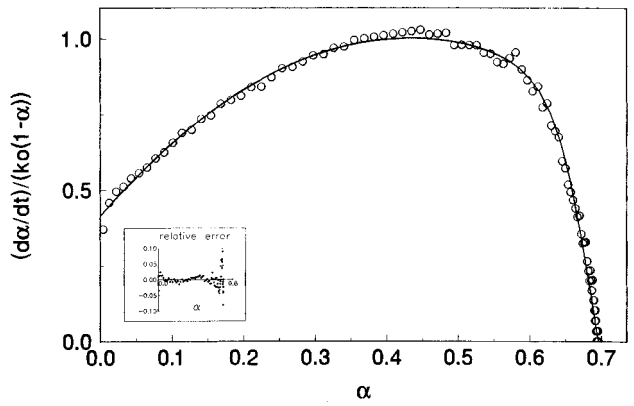

Figure 8. Normalized kinetic rate $k(\alpha)/k_0 = (d\alpha/dt)[1/(k_0(1-\alpha))]$ against the extent of reaction α for the cure of the system DGEBA-PACM at $T = 323$ K.

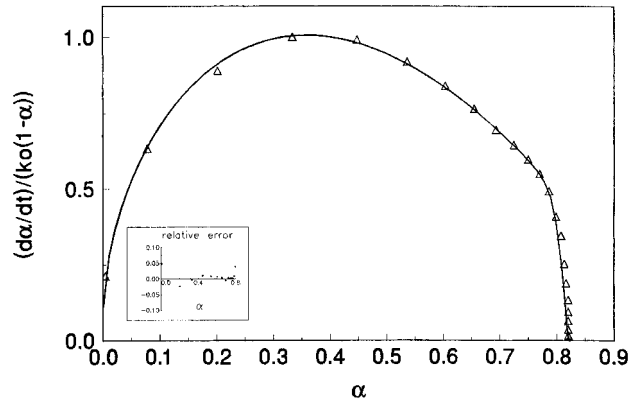

Figure 9. Normalized kinetic rate $k(\alpha)/k_0 = (d\alpha/dt)[1/(k_0(1-\alpha))]$ against the extent of reaction α for the cure of the system DGEBA−PACM at $T = 353$ K.

Table 2. Kinetic Parameters for the Diffusion Factor Expressed in Eq 17 Describing the Thermosetting of the DGEBA−PACM System[a]

T (K)	k_0 (min^{-1})	α_f	b	r
313	1.27×10^{-4}	0.659	0.017	0.990
323	1.96×10^{-4}	0.696	0.034	0.998
333	3.77×10^{-4}	0.747	0.032	0.991
353	1.50×10^{-3}	0.820	0.010	0.990

[a] T is the temperature of the cure, k_0 is the rate coefficient for the non-diffusion-controlled kinetic regime, α_f is the final degree of conversion of the epoxide−amine thermoset, b is an empirical constant, and r is the correlation coefficient between the experimental data and the theoretical curve corresponding to eq 17.

The kinetic parameters k_0, α_f, and b, corresponding to eqs 15 and 17, together with the correlation coefficient r for the later stages of the present diepoxide−diamine thermoset reaction at 313, 323, 333, and 353 K are summarized in Table 2. The rate coefficient k_0 was found to obey the following Arrhenius relationship, and a good linear correlation was observed ($r = 0.999$).

$$k_0 = A \exp(-E^{\ddagger}/RT) \tag{18}$$

We calculated $\ln(A) = 13.39$ and the apparent activation energy $E^{\ddagger} = 59$ kJ/mol. This energy value is similar to those obtained by Cole[17] and Chiao[18] for epoxide−amine reactions of different systems. In Table 2, α_f is seen to increase as the temperature of cure is increased. Cole[17] proposed a linear relationship of α_f against the temperature of the cure. However, this relationship is not valid outside the experimental temperature range. A better empirical equation to express α_f as a function of T was found to be

$$\alpha_f = 1.354 \ln(T) - 7.127 \qquad (r = 0.998) \tag{19}$$

Hence eq 19 gives a good approximation of the evolution of α_f over a larger range of temperature than a linear equation. The empirical constant b was expected to rise as the temperature of the cure was lowered, according to the theory that the reaction is slower at low temperature, and the network changes are also slower at the later stage of the cure. But the b values obtained from the analysis that are summarized in Table 2 do not follow such behavior. In further studies by us, it was concluded that no systematic trend with temperature was observed. The average value for b was 0.0232 with a standard variation $s = 1.16 \times 10^{-2}$.

It was interesting to incorporate our diffusion control term, eq 17, in a theoretical equation which completely describes the kinetics of the cure for all the temperatures. For temperatures below 333 K, the best fit was obtained by combining Horie's equation (13) with the diffusion control factor eq 17. In eq 13, the constant B is the ratio of primary amine N−H bonds to epoxide groups in the initial mixture. The chosen ratio of (diepoxide/diamine) was (2/1) so the value of B was 1. In this case, Horie's equation corresponds to Kamal's equation (14), with $m = 1$ and $n = 2$. These values of m and n were proposed by Riccardi[19] to fit the kinetics of an amine adduct cured DGEBA. Thus, only the reactions between the epoxide group, the primary amines, and the secondary amines have to be considered for these temperatures. In the first stage of curing, the kinetics are found to be second order with respect to epoxide groups, but in the later stage, first and second order can be assumed to be present as well. The incorporation of eq 17 in Horie's equation gives

$$\frac{d\alpha}{dt} = g(\alpha)f_d(\alpha) = k_0(k_1 + k_2\alpha)(1-\alpha)^2 \times \left[\frac{2}{1 + \exp\left(\frac{\alpha - \alpha_f}{b}\right)} - 1\right] \tag{20}$$

Figure 8 shows the excellent correlation between our experimental data and the theoretical fit using eq 20 for the cure of the DGEBA−PACM system at 323 K over the entire range of α. The kinetic rates k_0, k_1, and k_2, the constant b, and the correlation factor r are given in Table 3 for the epoxide−amine thermoset at three different curing temperatures. The values of the constant b are slightly different from those summarized in Table 2 because of the second-order rate of eq 20.

At 353 K, the experimental data were not fitted with eq 20, but a good result was obtained by a combination of Kamal's equation (14) (with $m = 0.6$ and $n = 2$) and the diffusion control factor (17), giving the following relation:

Table 3. Evaluation of the Kinetic Parameters of Eqs 20 and 21[a] for the Thermoset of the DGEBA−PACM System

T (K)	k_0 (min^{-1})	k_1	k_2	b	r
313	1.27×10^{-4}	0.306	3.073	0.0127	0.998
323	1.96×10^{-4}	0.415	3.124	0.0264	0.999
333	3.77×10^{-4}	0.346	3.233	0.0203	0.991
353	1.50×10^{-3}	0.110	2.697	0.0100	0.999

[a] Equation 20 was used to fit the data obtained during the cure of the thermoset DGEBA−PACM at 313, 323, and 333 K while eq 21 was used at 353 K.

$$\frac{d\alpha}{dt} = k_0(k_1 + k_2\alpha^{0.6})(1-\alpha)^2\left[\frac{2}{1+\exp\left(\frac{\alpha-\alpha_f}{b}\right)} - 1\right] \quad (21)$$

The correlation coefficient between this equation and the fit to the data obtained from the present experiments is $r = 0.999$; the curve using eq 21 and the experimental data for the cure at 353 K are drawn in Figure 9.

5. Discussion

During the epoxide−amine thermosetting reaction, irreversible changes in the physical properties are observed in both dielectric and DSC experiments as the extent of reaction α increases from zero to the final degree of conversion. We observe that an obvious correlation between DRS and DSC dynamics is possible, but is difficult to quantify during a reaction. Thus DRS measurements predict that if molecular motions, at a given reaction temperature T_R, have reached a time scale $t > 10^2$ s, then the material may be regarded operationally as a "glass". When the time scale for molecular motion reaches this region, then as the reaction proceeds, it is expected that the reaction would tend to be approaching the diffusion-controlled limiting range and would effectively "stop". Extrapolations of dielectric data at medium frequencies to the low-frequency range should give indications of the vitrification region in which polymerization actually stops (i.e. the rate of reaction becomes effectively zero). We shall examine, through comparisons of DRS and dynamic DSC data, the extent to which DRS can predict the kinetic behavior in the vitrification region and hence draw up a set of guidelines based on general working rules.

The present attempt to establish qualitative and quantitative relationships between the kinetic and dielectric behavior of an epoxide−amine thermoset curing requires careful consideration and a precise definition of terms. The relaxed permittivity ϵ_0, which is the short-term value of ϵ' for each plot in Figure 1a, was dependent on the concentration of the dipole chain segments in the initial mixture. The average dielectric relaxation time for molecular motions in the reacting mixture increases with the extent of reaction as the effective local viscosity increases. In our experimental range, the plots of log f_m vs t_m were linear, in accord with eq 8, at each reaction temperature. *In this analysis, as a working rule, we shall assume that such plots are linear within and beyond the ranges of f_m and T_R shown in Figure 10* and we shall use the values extrapolated to higher and lower frequencies as a part of a systematic method for comparison of DRS and DSC data. Clearly, the extremely low values of log(f_m) could not be observed experimentally but are predicted using the explicit assumption that we make in our systematic analysis. That forms a basis for the changes in f_m in the later stages of the diffusion-controlled range. The relationship between f_m and t_m shown in Figure 10 can be expressed by eq 22 derived from eq 8:

$$\log(f_m) = \log(f_m(0)) - \frac{kt_m}{\ln(10)} \quad (22)$$

where $f_m(0)$ is a temperature-dependent quantity and k is a rate coefficient summarized in Table 1. The semiempirical kinetics equations (20) and (21) were found to fit the whole range of experimental data at 313, 323, 333, and 353 K and can be rewritten as

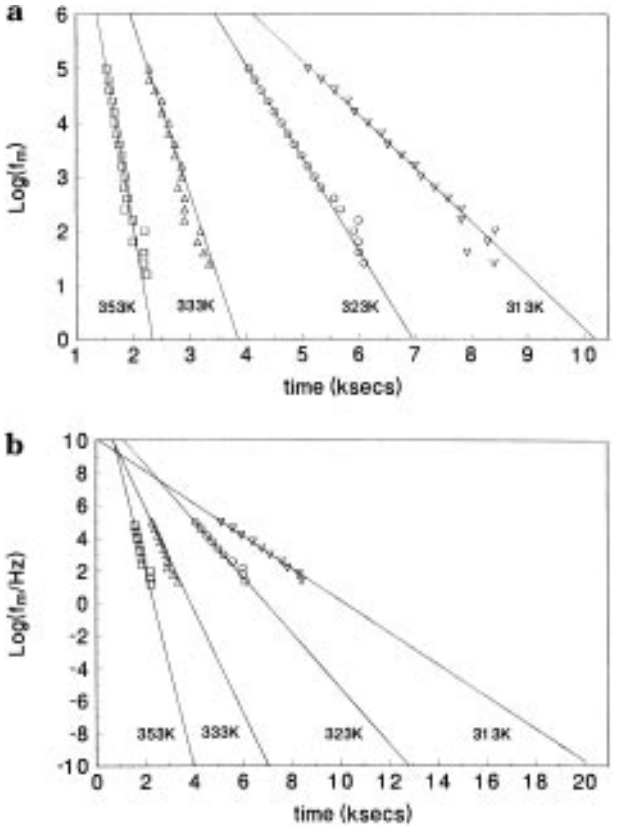

Figure 10. Frequency of maximum loss, on a logarithmic scale, against the time of reaction for the curing temperatures $T = 313$ K (▽), $T = 323$ K (○), $T = 333$ K (△), and $T = 353$ K (□).

$$\frac{d\alpha}{dt} = g(\alpha)f_d(\alpha) \quad (23)$$

where $f_d(\alpha)$ is the diffusion control factor expressed in eq 17 and $g(\alpha)$ is derived from Horie's equation (respectively Kamal's equation) that fit the normal kinetic regime data in eq 20 (respectively eq 21). The functional form of eq 23 allows us to calculate the time $t(\alpha)$ needed to reach a given extent of reaction by a numerical integration:

$$t(\alpha) = \int_0^\alpha \frac{d\alpha}{g(\alpha)f_d(\alpha)} \quad (24)$$

Thus according to eqs 22 and 24, the frequency of maximum loss f_m at which the dielectric absorption reaches its maximum at a fixed T_R can be expressed as a function of the degree of conversion of the reaction as follows:

$$\log(f_m) = \log(f_m(0)) - \frac{k}{\ln(10)}\int_0^\alpha \frac{d\alpha}{g(\alpha)f_d(\alpha)} \quad (25)$$

A different way to plot log(f_m) vs α is to use the DSC data which gives for each experimental extent of reaction the corresponding measurement time. Thus this time can be transformed with the aid of eq 24 in order to obtain the values of log(f_m) for all the values of α obtained through the DSC measurement. The plots of log(f_m) and $(d\alpha/dt)/(k_0(1-\alpha))$, which represents the normalized kinetic rate coefficient $k(\alpha)/k_0$, are drawn as a function of α in Figure 11 for $T = 333$ K. It appears

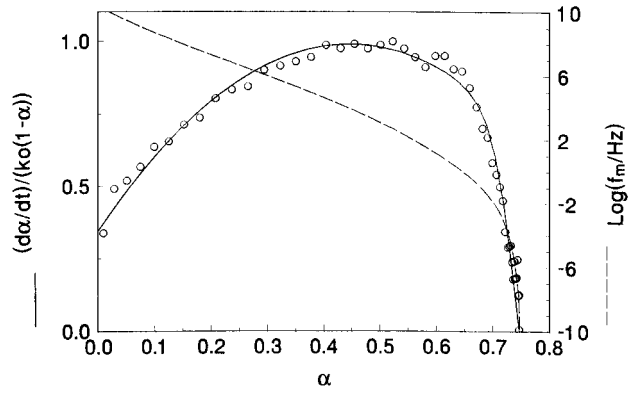

Figure 11. Normalized kinetic rate $k(\alpha)/k_0 = (d\alpha/dt)[1/(k_0(1 - \alpha))]$ against the extent of reaction α for the cure of the system DGEBA−PACM at $T = 333$ K. Also shown are $\log(f_m/\text{Hz})$ against α, where f_m is the frequency of maximum loss.

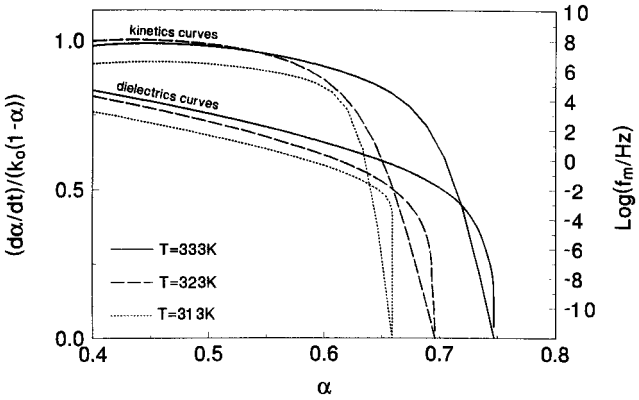

Figure 12. Normalized kinetic rate $k(\alpha)/k_0 = (d\alpha/dt)[1/(k_0(1 - \alpha))]$ against the extent of reaction α for the cure of the system DGEBA−PACM at $T = 333$ K (—), $T = 323$ K (– – –), and $T = 313$ K (•••). Also shown are $\log(f_m/\text{Hz})$ against α for comparison.

that the curves $\log(f_m)$ vs α are somewhat similar for all the cure temperatures $T \leq 333$ K, as seen in Figure 12. $\log(f_m)$ decreases approximately linearly as α increases in the range 0−0.6; then it drops suddenly to lower values as the reaction becomes diffusion controlled. The kinetics curves indicate the advent of the diffusion control when they decrease quickly in the latter stage of the reaction. Owing to this observation, we take as a reference that diffusion control becomes important at a fixed extent of reaction that we define as $\alpha/\alpha_f = 85\%$. This numerical value was also proposed by Enns and Gillham[25] as the characteristic extent of reaction for the conversion from *gel to glass*. This proposition required a comment. Indeed the gel is a network of limited stiffness which can be quantified by a modulus as distinct from a liquid of high viscosity whose modulus is zero. After a long observation time, the viscous liquid becomes a gel and then a glass. However, no characteristic state of the thermoset will be associated at the value of $\alpha = 0.85\alpha_f$ in this study, but for this extent of reaction, $\log(f_m)$ is found to be approximately equal to zero for the three curing temperatures considered. Reciprocally, for $\log(f_m) = 0$ the extents of reaction are found to be 86, 88, and 86% of α_f for respectively $T = 313$, 323, and 333 K. Considering Figure 12 and the observations above, the following *working rules* can therefore be established:

(i) The diffusion control of the reaction is characterized by the declination of the kinetic curves, which entails the sharp fall in the dielectric curves $\log(f_m)$ vs α. Now it appears in Figure 12 that for $\log(f_m) > 1$ and

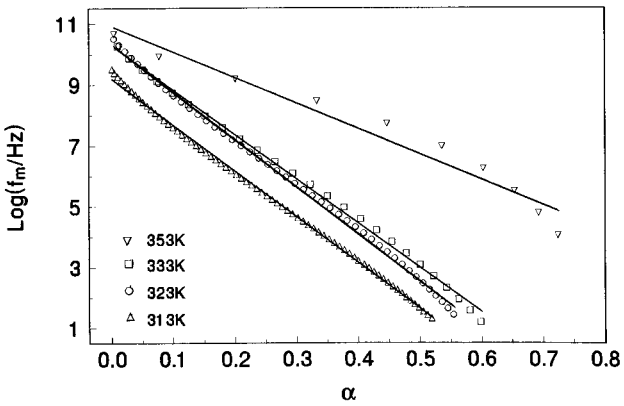

Figure 13. Frequency of maximum loss, on a logarithmic scale, against the extent of reaction α for the curing temperatures $T = 313$ K (△), $T = 323$ K (○), $T = 333$ K (□), and $T = 353$ K (▽).

$T = 313$, 323, and 333 K, the dielectric data points for our frequency range $10-10^5$ lie approximately on straight lines, which corresponds to a normal kinetic regime. This behavior can be seen in Figure 13, where, for our data, $\log(f_m)$ is drawn as a function of α for the normal kinetic range ($\alpha < 0.6$). Thus the reaction is *not diffusion controlled* at the time t_m when the dielectric loss peak occurs for every measurement frequency *in our range* ($10^{1.2}-10^5$ Hz). At $T = 333$ K for instance, when ϵ'' reach its maximum at $f = 10^5$ Hz, the value of α represents only 50% of the final degree of conversion and is 67% of α_f for $f = 10^3$ Hz. *Hence at low temperatures, the present definition of the time of maximum loss peak as an indicator of the onset of the vitrification should be reconsidered carefully.*

(ii) The time at which the diffusion control of the thermoset occurs can be defined operationally (for the reasons seen above) by dielectric spectroscopy as the time required for the loss factor to reach its maximum value for the measurement frequency $f = 1$ Hz in our experimental temperature range (313−333 K). For $T = 353$ K, the curve $\log(f_m)$ vs α is qualitatively different from those at 313, 323, 333 K insofar as the marked drop due to diffusion control occurs very close to α_f. It was determined that the extent of reaction is 84% for $\log(f_m) = 5$, 92% for $\log(f_m) = 3$, and around 98% for $\log(f_m) = 0$.

The curves $\log(f_m)$ vs α can be partially seen in Figure 13 for the range $0 < \alpha < 0.65$. They were obtained from the extrapolated lines presented in Figure 10b which fit the experimental data in the range $10^{1.2} < f_m < 10^5$. Then in the curves $\log(f_m)$ vs α drawn in the normal kinetic regime ($\alpha < 0.6$), the values of $\log(f_m)$ seem to be linearly dependent on α. So we may write in this regime

$$f_m(\alpha) = f'_m(0) \exp[-(k_p\alpha)] \qquad (26)$$

The values of $f'_m(0)$, k_p, and the correlation coefficient r are presented in Table 4 for different cure temperatures. A good agreement between eq 26 and the data is seen in Figure 13 for the lower temperatures. These parameters displayed in Table 4 can be combined with (i) data for α_f and (ii) the diffusion control function $f_d(\alpha)$ to predict $\log(f_m)$ vs α. Indeed eq 17, which describes the drop of the kinetic curves, can be used as a cut-off function to fit the curves $\log(f_m)$ vs α in the diffusion control region, where the constant b is chosen to be 0.01 for all the curves and $\alpha_f(T)$ is defined in eq 17. Then we can build a family of theoretical curves for $\log(f_m)$

Table 4. Calculation of Parameters Deriving from Eq 26 for the Thermoset of the DGEBA−PACM System[a]

T (K)	$f'_m(0)$ Hz	k_p	r
313	1.6×10^8	34.7	0.99
323	2.1×10^8	35.7	0.99
333	2.0×10^8	33.6	0.99
353	4.9×10^8	16.9	0.98

[a] T is the temperature of the cure, $f'_m(0)$ is the frequency of maximum loss for the noncured DGEBA−PACM mixture, k_p is the rate coefficient, and r is the linear correlation coefficient between the experimental data and the theoretical straight line presented in Figure 13.

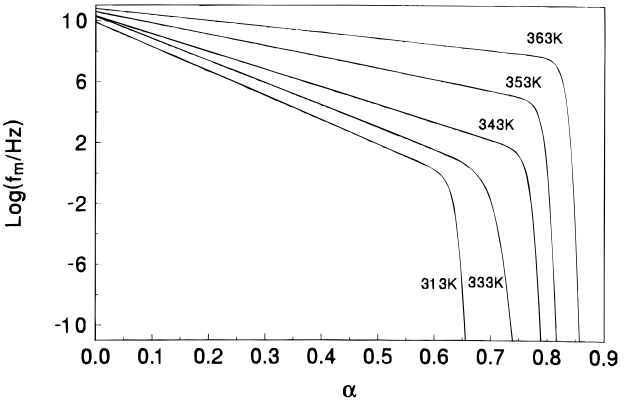

Figure 14. Theoretical plots of $\log(f_m/\text{Hz})$ against the extent of reaction α.

vs α, as shown in Figure 14 and corresponding to eq 27, for a fixed temperature of the cure:

$$\log(f_m(\alpha)) = a(T)\underbrace{\left[\log(f'_m(0)) - \frac{k\alpha}{\ln(10)}\right]}_{\text{A}} \times \underbrace{\left[\frac{2}{1+\exp\left[\frac{\alpha-\alpha_f(T)}{0.01}\right]} - 1\right]}_{\text{B}} + c(T) \quad (27)$$

In eq 27, the term A fits the data for $\log(f_m)$ in the range corresponding to the real kinetic regime. This part of the equation is based on the assumed linear dependence of $\log(f_m)$ with respect to time in the high-frequency domain. The term B is the cut-off function whose only variable is $\alpha_f(T)$. $a(T)$ and $c(T)$ are two temperature-dependent quantities which were extrapolated from the parameters summarized in Table 4. Figure 14 is only an approximate representation of the evolution of $\log(f_m)$ vs α during the cure of an epoxide−amine thermoset at different temperatures and it is based on the *working assumption* made here that $\log(f_m)$ is linearly dependent on t_m over a large range of frequencies, as presented in Figure 10b.

The curves presented in Figure 14 provide a general trend of the variation of $\log(f_m)$ as the extent of reaction increases and give some important information:

(i) The slopes of the straight lines $\log(f_m)$ vs α which form the theoretical model outside the diffusion-controlled regime are seen to decrease with increasing temperature of cure. At higher T_{cure}, the loss peak remains in the high-frequency domain until the effective vitrification process occurs, after which $\log f_m$ decreases rapidly.

(ii) In the diffusion-controlled range for fixed curing temperature, α is always very close to the value of α_f. We have taken as a reference $\log(f_m) = 0$ to define the onset of diffusion control at low cure temperature. Thus for $\log(f_m) < 0$, the diffusion controlled region is achieved at all the experimental temperatures and, according to Figure 14, we can consider that α_f is reached in practice.

We may make a quantitative correlation between the time-dependent dielectric relaxation process and the chemical kinetics over the whole range studied, and especially as the vitrification is approached and the reaction becomes diffusion controlled. The diffusion control limit and its temperature dependence are seen in Figure 14. As T_R increases, the pattern of the curves changes and the diffusion control sets in at successively higher frequencies. It was previously noticed that for $T_R < 333$ K, our experimental range of f_m ($10^{1.2}$−10^5 Hz) corresponded to the normal kinetic regime, but at 353 K, the dielectric loss peaks, occurring at time t_m for $f_m < 10^5$ Hz characterize the diffusion control region and then the final degree of conversion. Thus for high curing temperatures ($T > 353$ K), which are widely used in industry for epoxy−amine curing, it is possible to follow the extent of reaction in the vitrification region, by following the shift of the dielectric loss peak from high to low frequencies. The only data required to build the correlation curves in Figure 14 is the *final degree of conversion* of the network at the chosen temperature, which can be determined by DSC or FTIR measurements or also calculated with eq 8 in our case, or using another relationship for the kinetics, for example, that proposed by Cole.[17] Then by using a similar relation as eq 18, a set of correlation curves as shown in Figure 14 for our study, can be obtained for other systems.

6. Conclusions

We have made diverse comparisons between the dielectric data, for molecular dynamics, and the DSC data, for chemical kinetics, in order to understand how dielectric data can give information on the changes in kinetic behavior that lead to glass formation. The variation of the molecular dynamics over a large range of frequencies is complementary to the variation of the normalized kinetic rate coefficient $k(\alpha)/k_0(T)$ and has been studied here as a function of conversion $\alpha(t)$ for a given temperature. As the temperature is lowered, the loss peak measured in our frequency range does not occur in the diffusion-controlled kinetic regime, which obviously represents the effective vitrification of the network.

For temperatures above 353 K, at which epoxy−amine cures are usually performed, it is observed that the dielectric loss peak measured for any frequency in our experimental range coincides with the diffusion-controlled kinetic regime. In this case, the interpretation of the dielectric loss peak as the onset of the vitrification process, which has been widely used in the different studies of curing system, may be considered as valid. Our studies suggest that for all the curing temperatures studied, the reaction becomes diffusion controlled at times when the dielectric absorption described by $\epsilon''(t,f,L,T)$ reaches its maximum value ϵ''_{max} at measurement frequencies $f \leq 1$ Hz. This result should be considered as an quantitative indicator which relates the dielectric properties of the curing system to the real chemical changes in the thermoset.

Acknowledgment. We are pleased to acknowledge an Erasmus Grant to J.F. and thank Dr. John S. Davies for advice concerning the materials used in this study.

We thank EPSRC for their support of the dielectrics research group.

References and Notes

(1) McCrum, N. G.; Read, B. E.; Williams, G. *Anelastic and Dielectric Effects in Polymeric Solids*; Dover: New York, 1991.
(2) Ferry, J. D. *Viscoelastic Properties of Polymers*, 3rd ed.; Wiley: New York, 1980.
(3) Hill, N.; Vaugan, W.; Price, A. H.; Davies, M. *Dielectric Properties and Molecular Behaviour*; Van Nostrand: London, 1969.
(4) Williams, G. In *Comprehensive Polymer Science*, Allen, G., Bevington, J. C., Eds.; Pergamon: Oxford, 1989; Vol. 2, Chapter 7, p 601.
(5) Williams, G. In *Dielectric and Related Molecular Processes*; Specialist Periodical Reports; The Chemical Society: London, 1975; p 151.
(6) Sheppard, N. F.; Senturia, S. D. *Dielectric Analysis of Thermoset Cure*; *Adv. Polym. Sci.* **1986**, *80*, 1.
(7) Sheppard, N. F.; Senturia, S. D. *J. Polym. Sci., Part B: Polym. Phys.* **1989**, *27*.
(8) Mangion, M. B. M.; Johari, G. P. *Macromolecules* **1990**, *23*, 3687.
(9) Mangion, M. B. M.; Johari, G. P. *J. Polym. Sci., Part B: Polym. Phys.* **1990**, *28*, 71.
(10) Mangion, M. B. M.; Johari, G. P. *J. Polym. Sci., Part B: Polym. Phys.* **1990**, *28*, 1621.
(11) Mangion, M. B. M.; Johari, G. P. *Polymer* **1991**, *32*, 2747.
(12) Mangion, M. B. M.; Johari, G. P. *J. Polym. Sci., Part B: Polym. Phys.* **1991**, *29*, 437.
(13) Mangion, M. B. M.; Johari, G. P. *J. Polym. Sci., Part B: Polym. Phys.* **1991**, *29*, 1117.
(14) Mangion, M. B. M.; Johari, G. P. *J. Polym. Sci., Part B: Polym. Phys.* **1991**, *29*, 1127.
(15) Maistros, G. M.; Block, H.; Bucknall, C. B.; Partridge, I. K. *Polymer* **1992**, *33*, 4470.
(16) Cole, K. C. *Macromolecules* **1991**, *24*, 3093.
(17) Cole, K. C.; Hechler, J.-J.; Noël, D. *Macromolecules* **1991**, *24*, 3098.
(18) Chiao, L. *Macromolecules* **1990**, *23*, 1286.
(19) Carrozino, S.; Giovanni, L.; Rolla, P.; Tombari, E. *Polym. Eng. Sci.* **1990**, *30*, 366.
(20) Lane, J. W.; Seferis, J. C. *J. Appl. Sci.* **1986**, *31*, 1155.
(21) Mangion, M. B. M.; Wang, M.; Johari, G. P. *J. Polym. Sci., Part B: Polym. Phys.* **1992**, *30*, 445.
(22) Horie, K.; Hiuro, H.; Sawada, M.; Mita, I.; Kambe, H. *J. Polym. Sci., Part A-I* **1970**, *8*, 1357.
(23) Barton, J. M. *Adv. Polym. Sci.* **1985**, *72*, 111.
(24) Kamal, M. R. *Polym. Eng. Sci.* **1974**, *14*, 231.
(25) Enns, J. B.; Gillham, J. K. *J. Appl. Polym. Sci.* **1983**, *28*, 2567.

MA9517862